European Review for Medical and Pharmacological Sciences 2017; 21: 5072-5080

IGFBP2 induces SPRY1 expression via NF-κB signaling pathway in glioblastoma multiforme (GBM)

Z.-S. YUAN[1], Y. CAO[2], Z.-Y. LI[3]

[1]The 1st Department of Neurosurgery, The People's Hospital of Yinan, Yinan, Shandong, China
[2]Department of Orthopedics, The People's Hospital of Gaotang, Liaocheng, Shandong, China
[3]Department of Neurology, Weifang People's Hospital, Weifang, Shandong, China

Zhongshun Yuan and Yong Cao are co-first authors

Abstract. – OBJECTIVE: In this study, we aimed to investigate the downstream effector of IGFBP2 in glioblastoma multiforme (GBM) and its regulative effect on epithelial-to-mesenchymal transition (EMT) in GBM cells.

MATERIALS AND METHODS: Bioinformatics analysis was performed by using data in The Cancer Genome Atlas (TCGA)-GBM. Human GBM cell lines U87 and U251 cells were used as in vitro cell models to assess the influence of IGFBP2 on NF-κB activation and on SPRY1 expression. U251 cells were infected with SPRY1 shRNA. Then, the cells were subjected to Western blotting of mesenchymal markers and transwell assay of cell invasion.

RESULTS: IGFBP2 is significantly upregulated in GBM tissues than in normal brain tissues. High IGFBP2 expression is associated with poor overall survival (OS) (p=0.019) and poor progression free survival (PFS) among the patients (p=0.04). CpG island methylation phenotype (CIMP) is associated with a higher level of IGFBP2 DNA methylation and suppressed IGFBP2 expression. SPRY1 is co-upregulated with IGFBP2 (Pearson's r=0.51) in TCGA-GBM. IGFBP2 overexpression increased the expression of p-p65 and nuclear p65, while IGFBP2 knockdown reduced the expression of p-p65 and nuclear p65. In U251 cells, SPRY1 knockdown significantly reduced the expression of mesenchymal markers including N-cadherin, Vimentin, Snail and Twist1 and also impaired invasion capability of the cells.

CONCLUSIONS: IGFBP2 can induce SPRY1 expression via NF-κB signaling pathway in GBM cells. SPRY1 upregulation might be an important mechanism in the maintenance of mesenchymal phenotypes of GBM cells.

Key Words:
IGFBP2, SPRY1, NF-κB, Glioblastoma.

Introduction

Glioblastoma multiforme (GBM) is the most common form of malignant brain tumor[1,2]. Recent data from The Cancer Genome Atlas (TCGA) indicated that GBM tumors can be genetically divided into 4 subtypes: classical, mesenchymal, proneural, and neural[1]. Among these four subtypes, mesenchymal tumors are the most aggressive and are associated with the worst survival[1]. Epithelial-mesenchymal transition (EMT) is a biological process through which polarized epithelial cells obtain mesenchymal phenotypes[3]. During this transition, the cancer cells lose cell polarity and cell-cell adhesion, but acquire migratory and invasive properties[3]. Many studies showed that EMT is an important mechanism contributing to the invasiveness of high-grade GBM[4,5]. Therefore, understanding the mechanisms that drive EMT is crucial to identify potential therapeutic targets of GBM.

Insulin-like growth factor binding protein-2 (IGFBP2) is a secreted protein that binds IGF-I and IGF-II with high affinity[6]. IGFBP2 can also interact with many different ligands, independently of IGF binding[7]. Previous studies showed that IGFBP2 is significantly increased in GBM compared with low-grade gliomas and normal brain tissue[8,9]. Its upregulation directly promotes GBM stem cell expansion and survival[10] and positively correlates with GBM progression[9,11]. Knockdown of IGFBP2 induces GBM cell apoptosis and inhibits GBM cell migration and invasion[12,13]. However, the molecular mechanisms underlying its regulation in GBM are not well understood.

Corresponding Author: Zhenyan Li; e-mail: Zhenyanlee@hotmail.com

NF-κB family has 5 members, including p65/RelA, RelB, c-Rel, NF-κB1/p50, and NF-κB/p52l4. The dimer formed by p65 and p50 is the predominant form of NF-κBl4. Activation of this signaling pathway can promote mesenchymal differentiation of GBM cells and is strongly associated with GBM progression[15,16]. Sprouty (Spry) proteins are involved in multiple receptor tyrosine kinases (RTK) mediated MAPK/ERK signaling pathways, thereby contributing to the regulation of cell proliferation, migration, differentiation and apoptosis[17]. Sprouty 1 is encoded by SPRY1 gene and has paradoxical roles in different tumors. It has a potential tumor suppressive effect in prostate, ovarian and lung cancers[18-20], but shows an oncogenic effect in triple negative breast cancer[16]. These findings suggest that the role of SPRY1 might be cancer specific. However, its expression profile and functional role in GBM is not clear.

In this study, we found that IGFBP2 can induce SPRY1 expression via NF-κB signaling pathway in GBM cells. Knockdown of SPRY1 can reduce their mesenchymal properties.

Materials and Methods

Data Analysis of TCGA-GBM

IGFBP2 and SPRY1 mRNA expression in GBM tissues and in normal brain tissues were assessed using the FireBrowse (http://firebrowse.org/), a portal to cull and analyze data generated by TCGA. SPRY1 protein expression in GBM and in normal brain tissues was reviewed in the Human Protein Atlas (http://www.proteinatlas.org/)[21]. Kaplan-Meier curves of overall survival (OS)/progression free survival (PFS) in GBM patients were assessed by using R2: Genomics Analysis and Visualization Platform (http://r2.amc.nl), using data from TCGA-GBM. The patients were grouped by median IGFBP2 expression.

IGFBP2 expression, its DNA methylation status, CpG island methylation phenotype (CIMP) and isocitrate dehydrogenase 1 (IDH1) mutation status in TCGA-GBM, were examined using the UCSC Xena (http://xena.ucsc.edu/). Kaplan-Meier curves of OS in patients belonging to CIMP or non-CIMP group were generated. Log-rank test was used to assess the significance of difference between the curves.

Protein-Protein Interaction (PPI) Network Analysis

The genes co-upregulated with IGFBP2 (Pearson's $r \geq 0.5$) in TCGA-GBM were identified using the cBioPortal for Cancer Genomics (http://cbioportal.org)[22]. Then, the genes were loaded into the Search Tool for the Retrieval of Interacting Genes (STRING) (http://string-db.org/) database for identifying the known PPI network.

Cell Culture and Infection

Human GBM cell lines U87 and U251 were purchased from the Institute of Biochemistry and Cell Biology (Shanghai, China). Cells were cultured in Dulbecco's modified Eagle's medium (DMEM) supplemented with 10% fetal bovine serum (FBS, Invitrogen, Carlsbad, CA, USA) and antibiotics (100 U/ml penicillin and 100 μg/ml streptomycin) at 37°C in a humidified chamber with 5% CO_2.

Lentiviral IGFBP2 expression particles (PS100071) and the negative controls were obtained from OriGene (Rockville, MD, USA). Lentiviral IGFBP2 shRNA (sc-37195-V), SPRY1 shRNA (sc-41035-V) and the negative controls were purchased from Santa Cruz Biotechnology (Santa Cruz, CA, USA). U87 cells were infected with the expression particles for overexpression, while U251 cells were infected with the shRNA particles for knockdown. Infection was performed according to manufacturer's instruction.

Quantitative Real-time PCR (qPCR)

Total RNAs were extracted from cell samples using the RNeasy mini kit (Qiagen, Hilden, Germany). The samples with a ratio of 260 nm/280 nm absorption between 1.8 and 2.0 were used. Then, cDNA was synthesized by using the ProtoScript First Strand cDNA Synthesis kit (New England Biolabs, Ipswich, MA, USA). After that, qPCR was performed to detect the expression of target genes using the SYBR® Select Master Mix (Applied Biosystems, Foster City, CA, USA) in an ABI 7900HT Fast Real-time PCR System (Applied Biosystems). GAPDH was used as an internal reference in each reaction. The primers for IGFBP2 were: sense, 5'- GACAATGGCGATGACCACTCA-3' and antisense, 5'- GCTCCTTCATACCCGACTTGA-3' and for SPRY1 were: sense, 5'-GCCTTCTTTGGATAGCCGTCAG-3' and antisense, 5'-TCATTGCTGCCTCTTATGGCC-3'. The relative expression levels were calculated using the $2^{-\Delta\Delta CT}$ method.

Western Blotting

Cultured cell samples were lysed and homogenized in a lysis buffer with phosphatase

inhibitor and protease inhibitor cocktail. Then, equal amount of protein extracts were separated by electrophoresis on 10% sodium dodecyl sulphate-polyacrylamide gel electrophoresis (SDS-PAGE) and then were transferred to a nitrocellulose membrane. After washing, the membrane was blocked for 1 h in Tris-buffered saline containing 0.1% Tween 20 and 5% non-fat milk and then probed with primary bodies against IGFBP2 (ab4244, Abcam, Cambridge, MA, USA), NF-κB p-65 (Ab140751), p-p65 (s536) (ab86299, Abcam), Sprouty 1 (ab75492, Abcam), Vimentin (ab92547, Abcam), N-cadherin (ab12221, Abcam), Snail (ab53519, Abcam), Twist1 (ab50581, Abcam) and β-actin (ab3280, Abcam). Next, the membranes were washed and incubated with secondary antibodies conjugated to horseradish peroxidase (HRP). The immunoreactivity was revealed with Super Signal West Pico Chemiluminescent Substrate (Thermo Scientific, Waltham, MA, USA).

Transwell Assay of Cell Invasion

Cell invasion was determined by transwell assay using a Matrigel invasion chamber (BD Biosciences, Franklin Lakes, NJ, USA) in a 24-well cell culture plates according to the manufacturer's instruction. In brief, U251 cells (5×10^4 cells/mL) with or without infection of SPRY1 shRNA were seeded into chamber inserts containing an 8-μm pore size membrane with a thin layer Matrigel matrix, with 500 μl serum-free Dulbecco's Modified Eagle Medium (DMEM). The bottom of the well was filled with 700 μl DMEM medium with 20% fetal bovine serum (FBS). 48 h later, cells invaded to the lower surface of the membrane were fixed, while the non-invading cells on the upper surface were removed. The invaded cells were stained with 0.1% crystal violet and the number was then determined for 3 independent fields under a microscope.

Statistical Analysis

Data were presented as means and standard deviations (SDs). All analyses were performed with SPSS software package (Version 19.0, Armonk, NY, USA). Independent *t*-tests were used to compare the differences between two groups. One-way ANOVA with Bonferroni post-hoc test was performed to compare the differences between three or more groups. $p<0.05$ was considered statistically significant.

Results

IGFBP2 is Upregulated in GBM and its Upregulation is Associated with Poor OS and PFS

Data mining in FireBrowse showed that IGFBP2 is significantly upregulated in GBM tissues than in normal brain tissues (Figure 1A). Previous studies reported that IGFBP2 upregulation is associated with aggressive phenotypes of GBM[10,12]. To investigate the prognostic value of IGFBP2 in GBM, we further assessed the association between IGFBP2 expression and OS/PFS in TCGA-GBM. Results of the log-rank test showed that high IGFBP2 expression is associated with poor OS ($p=0.019$, Figure 1B) and also poor PFS among patients ($p=0.04$, Figure 1C).

IDH1 Mutation and CIMP are Associated with IGFBP2 Suppression in GBM

By data mining using the UCSC Xena, we generated a comparable heat map indicating the association among IGFBP2 expression, IDH1 mutation and CIMP in TCGA-GBM (Figure 2A). The results showed that CIMP is associated with a higher level of IGFBP2 DNA methylation and also suppressed IGFBP2 expression (Figure 2A). The correlation between CIMP and IDH1 mutation was also confirmed in the heat map (Figure 2A). IGFBP2 expression is significantly higher in non-Glioma-CIMP (non-G-CIMP) than in G-CIMP group (Figure 2B). Kaplan Meier curves indicated that the G-CIMP group has significantly better OS than the non-G-CIMP group ($p<0.001$, Figure 2C).

SPRY1 is Co-upregulated with IGFBP2 in GBM

IGFBP2 co-upregulated genes (Pearson's $r\geq0.5$) in TCGA-GBM were identified (Figure 3A). PPI network did not identify any known interactions between IGFBP2 and its co-upregulated genes (Figure 3B). In the PPI network, we found that SPRY1 is co-upregulated with IGFBP2 (Pearson's $r=0.51$, Figure 3C-D).

IGFBP2 Induces SPRY1 Expression via NF-κB Pathway in GBM Cells

Data mining in FireBrowse showed that SPRY1 is significantly upregulated in GBM tissues than in normal brain tissues (Figure 4A). IHC staining images obtained from the Human Protein Atlas revealed that SPRY1 expression is not detectable in glial cells and neuronal cells

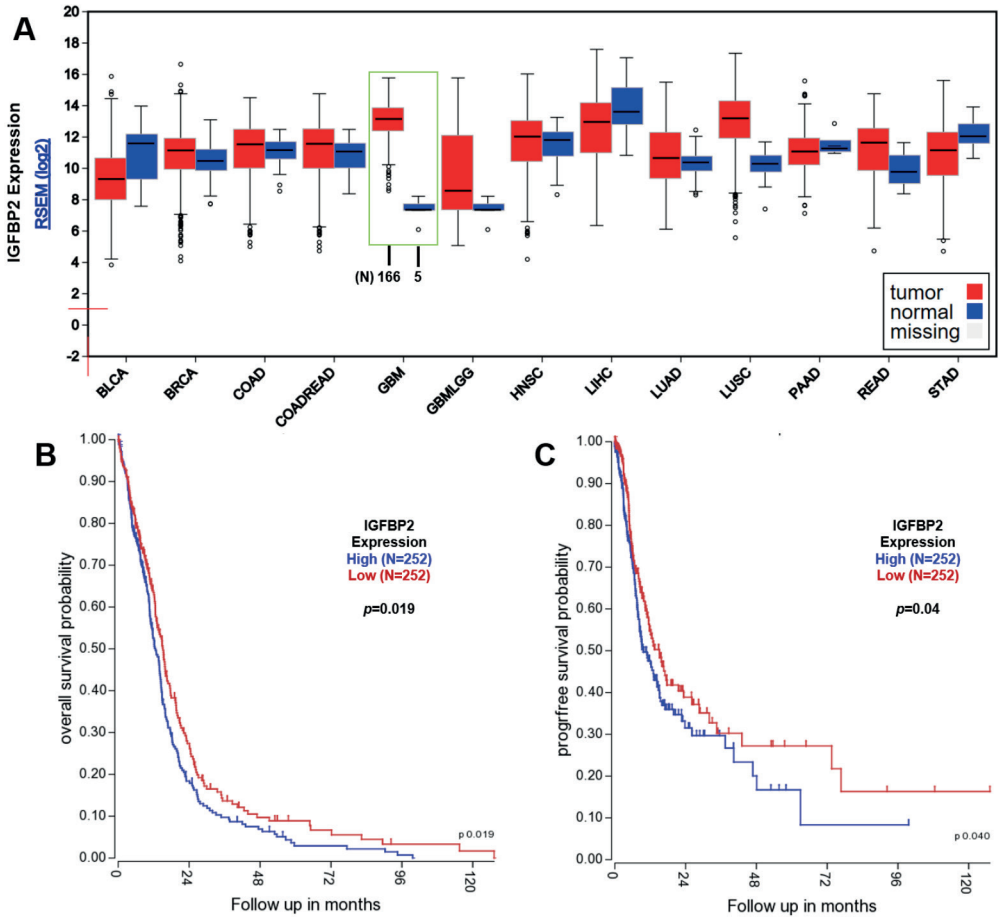

Figure 1. IGFBP2 is upregulated in GBM and its upregulation is associated with poor OS and PFS. ***A***, IGFBP2 mRNA expression in some solid tumors and in corresponding normal tissues. Data mining was performed using FireBrowse. ***B-C***, Kaplan-Meier curves of OS (B) and PFS (C) in patients with high or low IGFBP2 expression. The analysis was performed using R2 with data in TCGA-GBM. Survival curves were generated by setting median IGFBP2 expression as the cut-off.

in normal brain tissues (Figure 4B). However, the GBM tissue had moderate SPRY1 staining, which is expressed in both cytoplasm and membrane (Figure 4B). Then, U87 cells were infected with lentiviral IGFBP2 expression particles or the negative control, while U251 cells were infected with lentiviral IGFBP2 shRNA or the negative control (Figure 4C). IGFBP2 overexpression significantly increased SPRY1 expression (Figure 4D-E), while IGFBP2 knockdown significantly reduced SPRY1 expression (Figure 4D-E). SPRY1 expression can be activated by NF-κB signaling in multiple types of cancer[23,24]. In U87 cells, enforced IGFBP2 expression increased the expression of p-p65 and nuclear p65 (Figure 4E). In U251 cells, IGFBP2 knockdown reduced the expression of p-p65 and nuclear p65 (Figure 4E). These findings suggest that IGFBP2 can activate NF-κB signaling pathway in GBM cells.

SPRY1 Knockdown Partly Reverses EMT in GBM Cells

SPRY1 has a regulative effect on EMT in triple negative breast cancer[25]. In this study, we further investigated whether SPRY1 modulates EMT in GBM cells. U251 cells were firstly infected with SPRY1 shRNA (Figure 5A). SPRY1 knockdown significantly reduced the expression of mesenchymal markers including N-cadherin, Vimentin, Snail and Twist1 (Figure 5A). Following transwell assay showed that SPRY1 knockdown impaired invasiveness of U251 cells (Figure 5B).

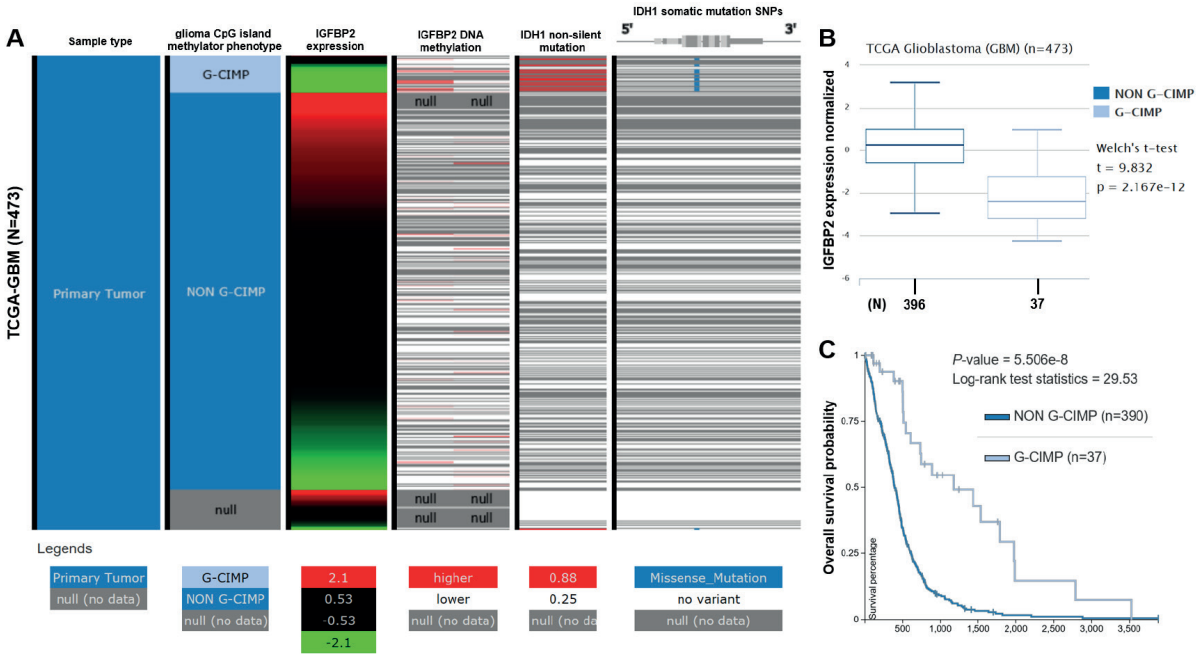

Figure 2. IDH1 mutation and CpG island methylation phenotype (CIMP) are associated with IGFBP2 suppression in GBM. ***A,*** Heat map of CIMP, IGFBP2 expression, IGFBP2 DNA methylation, and IDH1 mutation in TCGA-GBM. ***B,*** Box plots of IGFBP2 expression in non-G-CIMP and G-CIMP groups. ***C,*** Kaplan-Meier curves of OS in non-G-CIMP and G-CIMP patients. Data analysis was performed using the Xena Browser.

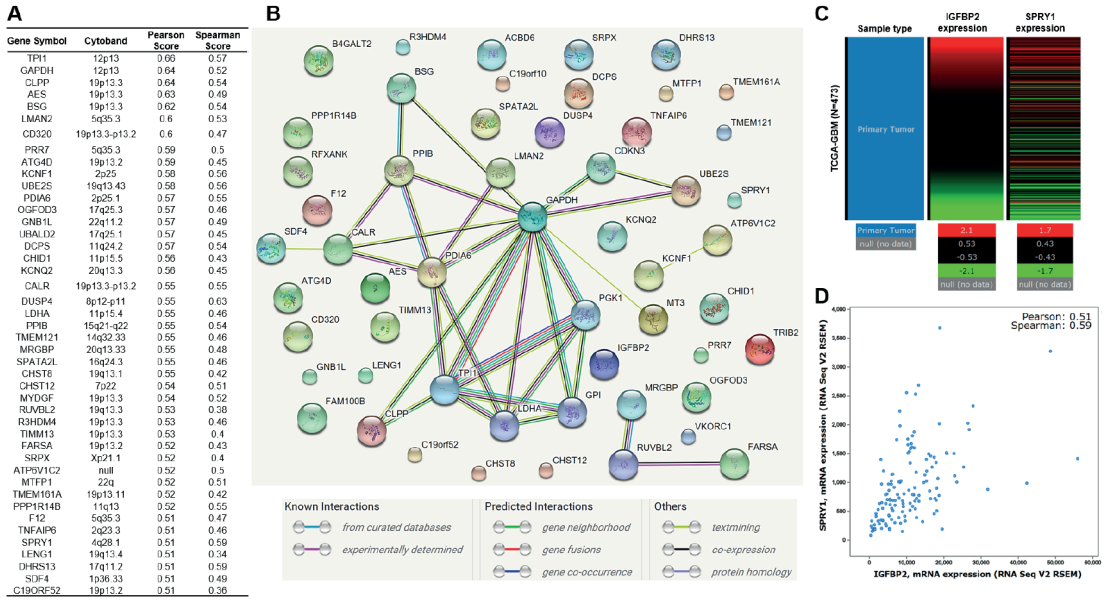

Gene Symbol	Cytoband	Pearson Score	Spearman Score
TPI1	12p13	0.66	0.57
GAPDH	12p13	0.64	0.52
CLPP	19p13.3	0.64	0.54
AES	19p13.3	0.63	0.49
BSG	19p13.3	0.62	0.54
LMAN2	5q35.3	0.6	0.53
CD320	19p13.3-p13.2	0.6	0.47
PRR7	5q35.3	0.59	0.5
ATG4D	19p13.2	0.59	0.45
KCNF1	2p25	0.58	0.56
UBE2S	19q13.43	0.58	0.56
PDIA6	2p25.1	0.57	0.55
OGFOD3	17q25.3	0.57	0.46
GNB1L	22q11.2	0.57	0.49
UBALD2	17q25.1	0.57	0.45
DCPS	11q24.2	0.57	0.54
CHID1	11p15.5	0.56	0.43
KCNQ2	20q13.3	0.56	0.45
CALR	19p13.3-p13.2	0.55	0.55
DUSP4	8p12-p11	0.55	0.63
LDHA	11p15.4	0.55	0.46
PPIB	15q21-q22	0.55	0.54
TMEM121	14q32.33	0.55	0.46
MRGBP	20q13.33	0.55	0.48
SPATA2L	16q24.3	0.55	0.46
CHST6	19q13.1	0.55	0.42
CHST12	7p22	0.54	0.51
MYDGF	19p13.3	0.54	0.52
RUVBL2	19q13.3	0.53	0.38
R3HDM4	19p13.3	0.53	0.46
TIMM13	19p13.3	0.53	0.4
FARSA	19p13.2	0.52	0.43
SRPX	Xp21.1	0.52	0.4
ATP6V1C2	null	0.52	0.5
MTFP1	22q	0.52	0.51
TMEM161A	19p13.11	0.52	0.42
PPP1R14B	11q13	0.52	0.55
F12	5q35.3	0.51	0.47
TNFAIP6	2q23.3	0.51	0.46
SPRY1	4q28.1	0.51	0.59
LENG1	19q13.4	0.51	0.34
DHRS13	17q11.2	0.51	0.59
SDF4	1p36.33	0.51	0.49
C19ORF52	19p13.2	0.51	0.36

Figure 3. IGFBP2 is co-upregulated with SPRY1 in GBM. ***A,*** The genes co-upregulated with IGFBP2 in TCGA-GBM (Pearson's r >0.5). The analysis was performed using the cBioPortal for Cancer Genomics. ***B,*** Protein-Protein Interaction (PPI) network among IGFBP2 and its co-upregulated genes. ***C-D,*** Heap map and regression analysis of the correlation between IHFBP2 and SPRY1 in TCGA-GBM.

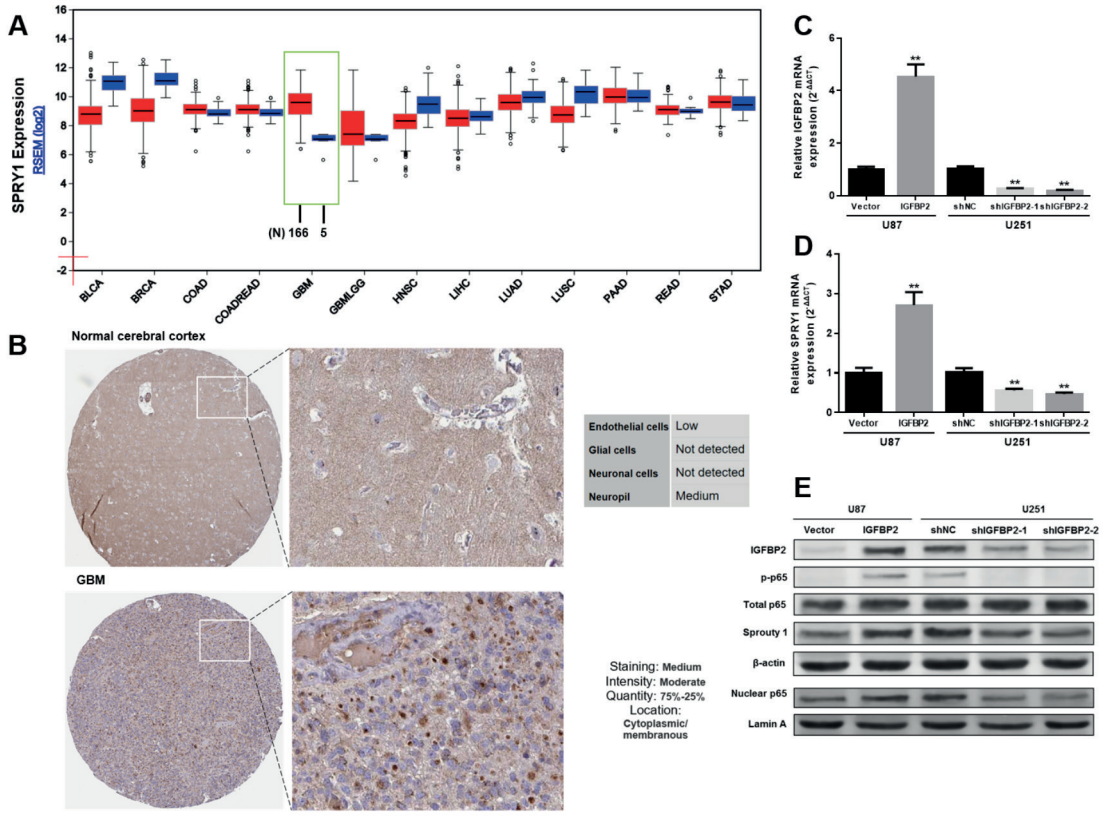

Figure 4. IGFBP2 induces SPRY1 expression via NF-κB pathway in GBM cells. ***A,*** SPR1 mRNA expression in some solid tumors and in corresponding normal tissues. Data mining was performed using FireBrowse. ***B,*** IHC staining of SPRY1 expression in normal cerebral cortex and GBM tissues. Images were obtained from the Human Protein Atlas (http://www.proteinatlas.org/search/SPRY1). ***C-D,*** QRT-PCR analysis of IGFBP2 (C) and SPRY1 (D) mRNA expression in U87 36 h after infection of IGFBP2 expression particles or the negative control or in U251 cells 36 h after infection of IGFBP2 shRNA or the negative control. ***E,*** Western blot analysis of IGFBP2, p-p65, total p65, nuclear p65 and Sprouty 1 expression in U87 and U251 cells 48 h after indicated infection in Figure C. **, $p<0.01$.

Discussion

In this study, by analysis of data in TCGA-GBM, we confirmed significantly upregulated IGFBP2 in GBM tissues than in normal tissues. In addition, we also observed that high IGFBP2 expression is associated with poor OS and poor PFS among the patients. However, the mechanism of IGFBP2 dysregulation in GBM is largely unknown. IDH1 mutation is the molecular basis of CIMP and both phenotypes are favorable prognostic biomarkers in patients with GBM[26]. In fact, CIMP is closely related to hypermethylation of a vast number of genes[27]. Therefore, we tried to investigate whether the expression of IGFBP2 is related to CIMP in GBM. Results of the bioinformatics analysis indicated that CIMP is associated with a higher level of IGFBP2 DNA methylation and suppressed IGFBP2 expression. These findings suggest that hypomethylation might be an important mechanism of aberrant IGFBP2 expression in GBM patients. Previous researches indicate that IGFBP2 can enhance GBM invasion by activating invasion-enhancing genes, including MMP2[8] and ADAMTS1[11]. In fact, besides binding with IGF, IGFBP2 can also interact with many different ligands, thereby modulating several signaling pathways. For example, IGFBP2 can bind with integrins[12] and NF-κB[28] and can also potentiate nuclear EGFR-STAT3 signaling[7], thereby activating the corresponding downstream genes. To further explore the downstream regulation of IGFBP2, we identified its co-expressed genes in TCGA-GBM. By performing PPI network analysis, we found that the mechanisms underlying their association are largely unknown. In the network, we observed that SPRY1 is significantly co-upregulated with IGFBP2. SPRY1 activation in some tissues is NF-κB dependent[23,24]. Inhibition of NF-κB activation can decrease SPRY1 expression[23]. Therefore, we

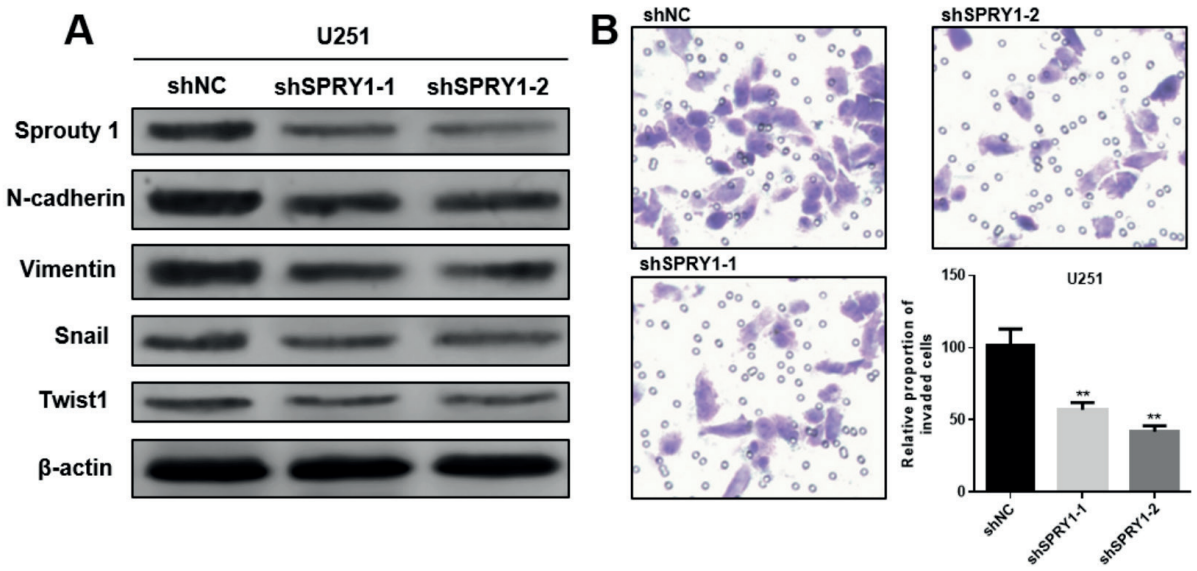

Figure 5. SPRY1 knockdown partly reverses EMT in GBM cells. ***A,*** Western blot analysis of Sprouty 1, N-cadherin, Vimentin, Snail and Twist1 expression in U251 cells 48 h after infection of SPRY1 shRNA. ***B,*** Representative images and quantitation of invaded U251 cells with or without SPRY1 knockdown. **, $p<0.01$.

suggested that IGFBP2 might induce SPRY1 expression via activating NF-κB signaling pathway. By using GBM U87 and U251 cells, we found that IGFBP2 overexpression increased the expression of p-p65 and nuclear p65, while IGFBP2 knockdown reduced the expression of p-p65 and nuclear p65. These findings have confirmed that IGFBP2 can activate NF-κB signaling pathway in GBM cells. In combination with previous investigations, we infer that IGFBP2 can induce SPRY1 expression via NF-κB signaling pathway in GBM cells. Previous studies reported that SPRY1 can inhibit neural differentiation in mouse embryonic stem cells, while SPRY1 inhibition can promote neural differentiation of mouse embryonic stem cells[29]. In addition, SPRY1, together with SPRY2, act as negative feedback regulators of FGF signaling, thereby inhibiting neurogenesis and progenitor cells maturation[30]. These findings suggest that SPRY1 is an essential gene maintaining stem cell properties of neural progenitor cells. In triple negative breast cancer cell line MDA-MB-231 cells, SPRY1 knockdown increased epithelial phenotype of the cells and reduced cell migration, Matrigel invasion, and anchorage-dependent and -independent growth[25]. In addition, SPRY1 knockdown also resulted in suppressed Snail and Slug expression[25], suggesting that SPRY1 plays a key role in mesenchymal phenotypes of the cancer cells. In U251 cells, we confirmed that SPRY1 knockdown significantly reduced the expression of mesenchymal markers including N-cadherin, Vimentin, Snail and Twist1 and impaired their invasion capability. Therefore, we infer that SPRY1 upregulation might be an important mechanism in the maintenance of mesenchymal phenotypes of GBM cells.

Conclusions

IGFBP2 can induce SPRY1 expression via NF-κB signaling pathway in GBM cells. SPRY1 upregulation might be an important mechanism in the maintenance of mesenchymal phenotypes of GBM cells.

Conflict of interest

The authors declare no conflicts of interest.

References

1) Kloosterhof NK, De Rooi JJ, Kros M, Eilers PH, Sillevis Smitt PA, Van Den Bent MJ, French PJ. Molecular subtypes of glioma identified by genome-wide methylation profiling. Genes Chromosomes Cancer 2013; 52: 665-674.

2) Jiang J, Lan YQ, Zhang T, Yu M, Liu XY, Li LH, Chen XP. The in vitro effects of caffeine on viability, cycle cycle profiles, proliferation, and apoptosis of

glioblastomas. Eur Rev Med Pharmacol Sci 2015; 19: 3201-3207.

3) Iser IC, Pereira MB, Lenz G, Wink MR. The epithelial-to-mesenchymal transition-like process in glioblastoma: an updated systematic review and in silico investigation. Med Res Rev 2017; 37: 271-313.

4) Zhu T, Li X, Luo L, Wang X, Li Z, Xie P, Gao X, Song Z, Su J, Liang G. Reversion of malignant phenotypes of human glioblastoma cells by beta-elemene through beta-catenin-mediated regulation of stemness-, differentiation- and epithelial-to-mesenchymal transition-related molecules. J Transl Med 2015; 13: 356.

5) Guo E, Wang Z, Wang S. MiR-200c and miR-141 inhibit ZEB1 synergistically and suppress glioma cell growth and migration. Eur Rev Med Pharmacol Sci 2016; 20: 3385-3391.

6) Fuller GN, Rhee CH, Hess KR, Caskey LS, Wang R, Bruner JM, Yung WK, Zhang W. Reactivation of insulin-like growth factor binding protein 2 expression in glioblastoma multiforme: a revelation by parallel gene expression profiling. Cancer Res 1999; 59: 4228-4232.

7) Chua CY, Liu Y, Granberg KJ, Hu L, Haapasalo H, Annala MJ, Cogdell DE, Verploegen M, Moore LM, Fuller GN, Nykter M, Cavenee WK, Zhang W. IGFBP2 potentiates nuclear EGFR-STAT3 signaling. Oncogene 2016; 35: 738-747.

8) Wang H, Wang H, Shen W, Huang H, Hu L, Ramdas L, Zhou YH, Liao WS, Fuller GN, Zhang W. Insulin-like growth factor binding protein 2 enhances glioblastoma invasion by activating invasion-enhancing genes. Cancer Res 2003; 63: 4315-4321.

9) Moore LM, Holmes KM, Smith SM, Wu Y, Tchougounova E, Uhrbom L, Sawaya R, Bruner JM, Fuller GN, Zhang W. IGFBP2 is a candidate biomarker for Ink4a-Arf status and a therapeutic target for high-grade gliomas. Proc Natl Acad Sci U S A 2009; 106: 16675-16679.

10) Hsieh D, Hsieh A, Stea B, Ellsworth R. IGFBP2 promotes glioma tumor stem cell expansion and survival. Biochem Biophys Res Commun 2010; 397: 367-372.

11) Martino-Echarri E, Fernandez-Rodriguez R, Bech-Serra JJ, Plaza-Calonge Mdel C, Vidal N, Casal C, Colome N, Seoane J, Canals F, Rodriguez-Manzaneque JC. Relevance of IGFBP2 proteolysis in glioma and contribution of the extracellular protease ADAMTS1. Oncotarget 2014; 5: 4295-4304.

12) Patil SS, Railkar R, Swain M, Atreya HS, Dighe RR, Kondaiah P. Novel anti IGFBP2 single chain variable fragment inhibits glioma cell migration and invasion. J Neurooncol 2015; 123: 225-235.

13) Lee CC, Chen PH, Ho KH, Shih CM, Cheng CH, Lin CW, Cheng KT, Liu AJ, Chen KC. The microRNA-302b-inhibited insulin-like growth factor-binding protein 2 signaling pathway induces glioma cell apoptosis by targeting nuclear factor IA. PLoS One 2017; 12: e0173890.

14) Hoffmann A, Leung TH, Baltimore D. Genetic analysis of NF-kappaB/Rel transcription factors defines functional specificities. EMBO J 2003; 22: 5530-5539.

15) Bhat KP, Balasubramaniyan V, Vaillant B, Ezhilarasan R, Hummelink K, Hollingsworth F, Wani K, Heathcock L, James JD, Goodman LD, Conroy S, Long L, Lelic N, Wang S, Gumin J, Raj D, Kodama Y, Raghunathan A, Olar A, Joshi K, Pelloski CE, Heimberger A, Kim SH, Cahill DP, Rao G, Den Dunnen WF, Boddeke HW, Phillips HS, Nakano I, Lang FF, Colman H, Sulman EP, Aldape K. Mesenchymal differentiation mediated by NF-kappaB promotes radiation resistance in glioblastoma. Cancer Cell 2013; 24: 331-346.

16) Gray GK, Mcfarland BC, Nozell SE, Benveniste EN. NF-kappaB and STAT3 in glioblastoma: therapeutic targets coming of age. Expert Rev Neurother 2014; 14: 1293-1306.

17) Walsh AM, Kapoor GS, Buonato JM, Mathew LK, Bi Y, Davuluri RV, Martinez-Lage M, Simon MC, O'Rourke DM, Lazzara MJ. Sprouty2 drives drug resistance and proliferation in glioblastoma. Mol Cancer Res 2015; 13: 1227-1237.

18) Shen L, Ling M, Li Y, Xu Y, Zhou Y, Ye J, Pang Y, Zhao Y, Jiang R, Zhang J, Liu Q. Feedback regulations of miR-21 and MAPKs via Pdcd4 and Spry1 are involved in arsenite-induced cell malignant transformation. PLoS One 2013; 8: e57652.

19) Masoumi-Moghaddam S, Amini A, Wei AQ, Robertson G, Morris DL. Sprouty 1 predicts prognosis in human epithelial ovarian cancer. Am J Cancer Res 2015; 5: 1531-1541.

20) Fritzsche S, Kenzelmann M, Hoffmann MJ, Muller M, Engers R, Grone HJ, Schulz WA. Concomitant down-regulation of SPRY1 and SPRY2 in prostate carcinoma. Endocr Relat Cancer 2006; 13: 839-849.

21) Lindskog C. The potential clinical impact of the tissue-based map of the human proteome. Expert Rev Proteomics 2015; 12: 213-215.

22) Cerami E, Gao J, Dogrusoz U, Gross BE, Sumer SO, Aksoy BA, Jacobsen A, Byrne CJ, Heuer ML, Larsson E, Antipin Y, Reva B, Goldberg AP, Sander C, Schultz N. The cBio cancer genomics portal: an open platform for exploring multidimensional cancer genomics data. Cancer Discov 2012; 2: 401-404.

23) Sabatel C, Cornet AM, Tabruyn SP, Malvaux L, Castermans K, Martial JA, Struman I. Sprouty1, a new target of the angiostatic agent 16K prolactin, negatively regulates angiogenesis. Mol Cancer 2010; 9: 231.

24) Mao XH, Chen M, Wang Y, Cui PG, Liu SB, Xu ZY. MicroRNA-21 regulates the ERK/NF-kappaB signaling pathway to affect the proliferation, migration, and apoptosis of human melanoma A375 cells by targeting SPRY1, PDCD4, and PTEN. Mol Carcinog 2017; 56: 886-894.

25) He Q, Jing H, Liaw L, Gower L, Vary C, Hua S, Yang X. Suppression of Spry1 inhibits triple-negative breast cancer malignancy by decreasing EGF/EGFR mediated mesenchymal phenotype. Sci Rep 2016; 6: 23216.

26) Hartmann C, Hentschel B, Wick W, Capper D, Felsberg J, Simon M, Westphal M, Schackert G, Mey-

ERMANN R, PIETSCH T, REIFENBERGER G, WELLER M, LOEFFLER M, VON DEIMLING A. Patients with IDH1 wild type anaplastic astrocytomas exhibit worse prognosis than IDH1-mutated glioblastomas, and IDH1 mutation status accounts for the unfavorable prognostic effect of higher age: implications for classification of gliomas. Acta Neuropathol 2010; 120: 707-718.

27) TURCAN S, ROHLE D, GOENKA A, WALSH LA, FANG F, YILMAZ E, CAMPOS C, FABIUS AW, LU C, WARD PS, THOMPSON CB, KAUFMAN A, GURYANOVA O, LEVINE R, HEGUY A, VIALE A, MORRIS LG, HUSE JT, MELLINGHOFF IK, CHAN TA. IDH1 mutation is sufficient to establish the glioma hypermethylator phenotype. Nature 2012; 483: 479-483.

28) HOLMES KM, ANNALA M, CHUA CY, DUNLAP SM, LIU Y, HUGEN N, MOORE LM, COGDELL D, HU L, NYKTER M, HESS K, FULLER GN, ZHANG W. Insulin-like growth factor-binding protein 2-driven glioma progression is prevented by blocking a clinically significant integrin, integrin-linked kinase, and NF-kappaB network. Proc Natl Acad Sci U S A 2012; 109: 3475-3480.

29) JUNG JE, MOON SH, KIM DK, CHOI C, SONG J, PARK KS. Sprouty1 regulates neural and endothelial differentiation of mouse embryonic stem cells. Stem Cells Dev 2012; 21: 554-561.

30) FAEDO A, BORELLO U, RUBENSTEIN JL. Repression of Fgf signaling by sprouty1-2 regulates cortical patterning in two distinct regions and times. J Neurosci 2010; 30: 4015-4023.